MULTIPLE DIPOLE HEART MODEL AND ITS PROJECTION TO THE BODY SURFACE POTENTIAL MAP

J. Švehlíková, M. Tyšler, M. Turzová

Institute of Measurement Science, Slovak Academy of Sciences, Bratislava, Slovakia

Abstract

We investigated the properties of a transfer matrix for the formulation of forward problem of electrocardiography, assuming the multiple dipole model of the generator of heart electrical activity (multiple dipole heart model). We used singular value decomposition (SVD) for factorization of the transfer matrix, paying special attention to its numerical null and signal spaces. The possibility of inverse reconstruction of the modeled multiple-dipole-equivalent source model of the heart electrical activity was studied. We used the angle between the source vector and its projection onto the transfer matrix signal space as a measure quantifying feasibility of finding the inverse solution.
Small ischemic lesions were modeled in selected heart regions by shortening the action potential duration by 20%. The derived theoretical results were tested for the multiple dipole heart model representing small ischemic lesions located on the endocardium and epicardium of modeled left ventricle.
It was shown that the theoretically best inverse result depended only on the formulation of the source model. As predicted, the best inverse solution was found for those lesions, which could be modeled by the source generator with the largest projection to the signal space of the transfer matrix.

1 Introduction

Presently, besides the classical 12-leads electrocardiograms (ECG), body surface potential maps (BSPM) recorded by multiple lead recording systems are available. Several model-based methods are used to understand and interpret the measured data. Various types of models of heart and torso configuration have been developed. They can vary from simple eccentric spheres [1] to realistically shaped heart and torso geometry, constructed from MRI scans. Similarly, the models of equivalent electric cardiac generator have been described by various approximations: a single dipole model, a multiple-dipole model, an epicardial source formulation [2] or a transmembrane potential source formulation [3]. The forward problem of electrocardiology concerns computation of body surface potential maps using the chosen model of heart generator and a transfer matrix. The transfer matrix is defined by properties of the torso as a volume conductor and the method of computation of the surface potentials. Regardless of the complexity of the model generator, the final set of forward problem equations after discretization often yields a linear equation **A.s=p**, where **A** is the transfer matrix, **s** represents the sources (heart generator) and **p** describes the measured potentials on the body surface [2],[4]. Forward simulations provide an effective tool for the verification of inverse reconstruction of equivalent model of electric generator from data measured on the torso surface. In the case of linear forward model formulation, solving the inverse problem leads to the computation of inverse of the transfer matrix **A,** which is usually non - regular), so the problem is ill-posed [4]. Small noise in the measured data can cause considerable

changes in the inverse solution. Another problem is non-uniqueness of the solution due to positive dimensionality of the transfer matrix null space [5].
In this paper multiple dipole equivalent model of the source of cardiac electrical activity was examined. The geometry of the heart ventricles was analytically defined by ellipsoids. Action potential propagation was modeled using the cellular automaton principle. The possibility of inverse reconstruction of multiple dipole model of heart generator representing small ischemic lesions was investigated. In the inverse solution, various levels of a criterion for truncated SVD of the transfer matrix were studied.

2 Materials and Methods

2.1 Model of multiple dipole heart generator

In the used model, real geometry of heart was replaced by its analytically described approximation by parts of ellipsoids, which constitute the ventricles and the epicardium [6] (Fig.1).

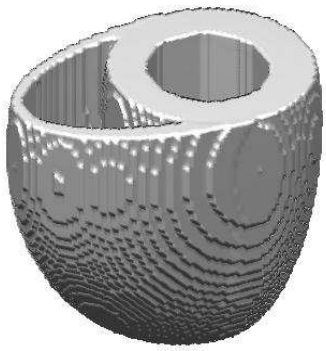

Fig.1. Analytically described model of heart ventricles

The modeled heart volume was divided into $1mm^3$ cubes, representing basic volume elements for the simulation of electrical activation propagation. It was assumed that every element consisted of the same type of cardiac cells with predefined shape and duration of action potential (AP). Five types of normal action potential duration, depending on the position of the volume element in the myocardium were considered: from 309 ms on the endocardium to 252 ms on the epicardium.
The spread of activation through the myocardium was initiated from 7 starting points selected according to the Durrer's investigations [7]. The activation progressed following the principles of cellular automaton, i.e. in each time step each element was activated from its neighbour. The velocity of the activation spread in most endocardial elements was 3-times higher, thus simulating the properties of Purkynje fibres. In Fig.2, isochrones for modeled normal activation in 3 cross-sections of the myocardium are displayed.

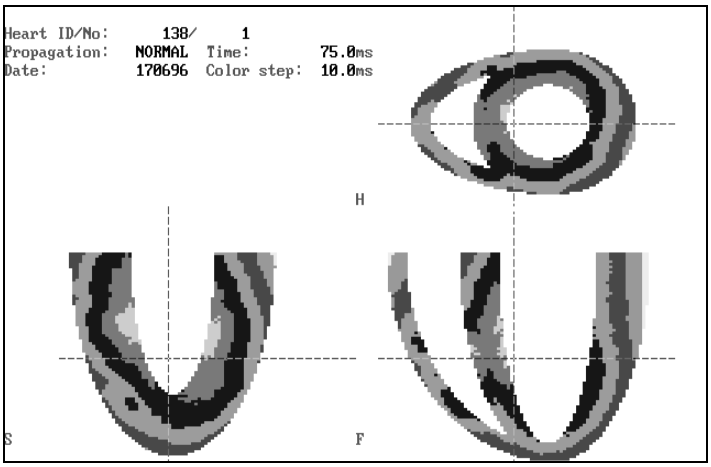

Fig.2. Isochrone maps for modeled normal spread of activation in 3 cross-sections of myocardium (H-horizontal, S-sagital, F-frontal).

In each time step an elementary current dipole was computed as the result of the difference between action potentials of adjacent volume elements. The modeled heart volume was divided into 168 segments, which created the resulting multiple dipole generator [6]. The elementary current dipoles belonging to each segment were then summed up and assigned to a corresponding representative point in the gravity center of the segment.

2.2 Forward simulations

For the forward problem solution, i.e. for the computation of potential maps on the model of human torso, we assumed that the modeled cardiac electric generator was inserted into a realistically shaped torso. The torso created the boundary between the volume conductor (the body) and an outer non-conductive medium. We also included the lungs and heart cavities as the main inhomogeneities **(**Fig. 3). The conductivity of lungs was set to be 4-times lower and the conductivity of blood in ventricles to be 3-times higher than the average conductivity of the torso [8].

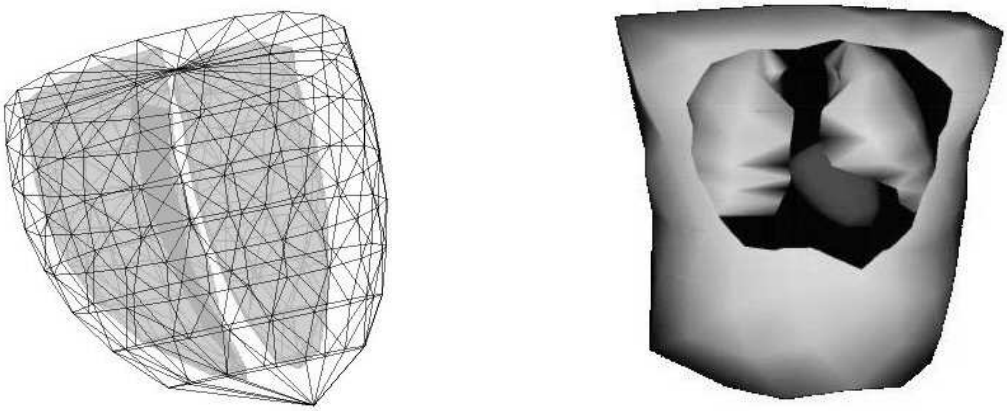

Fig.3. The model of heart surface with ventricles filled with blood (left). Realistically shaped torso and lungs used for forward simulations (right).

Assuming the above mentioned multiple dipole generator and applying the boundary element method (BEM) yielded the linear matrix equation**:**

$$\mathbf{A}.\ \mathbf{s} = \mathbf{p}, \qquad (1)$$

where **A** is the transfer matrix, **s** is the source vector and **p** is the vector of computed potentials on the torso. The coefficients of the transfer matrix were computed separately for

each component of each dipole of the generator. Having **n measured points** on torso and **m segmental dipoles** as generators, the dimensions of the components in the equation were as follows: **A** [n x (3m)] , **s**[(3m) x 1] , **p**[n x 1].
Because of the simplicity of the model, we used the model only in situations where such simplification may be appropriate, namely to model small ischemic lesions manifested during the phase of repolarisation.

2.3 Multiple dipole model of small ischemic lesions

Our modeling and simulation of small ischemic lesions was based on several assumptions: First, we assumed, that local ischemic disease manifests itself by the changes of action potential amplitude and duration. We modeled this situation by shortening and lowering the AP of the cardiac generator volume elements [9]. Second, we assumed that these changes cause typical baseline shifts in measured ECG signal, especially on the T wave. Time integral of surface potentials over the whole QRST interval depends only on the shape and amplitude of action potentials and not on the activation sequence. If we compute an integral map for a normal activation and then for an activation changed by ischemic disease, we can consider their difference **Δp** (difference integral map) to be the manifestation of the affected region of heart [10], [11].
We created several ischemic lesions by shortening the APs by 20 % in selected areas typical for the stenosis of main coronary vessels (Fig. 4) : lesion A – in the antero-septal part of left ventricle near the heart apex (supplied by the left anterior descending coronary artrery, LAD), lesion P – in the postero-lateral part of left ventricle close to the heart base (supplied by the circumflex coronary artery, Cx) and lesion I – inferior, in the mid postero-septal part of left and right ventricle (supplied by the right coronary artery, RCA). In each position we simulated 3 sizes of subendocardial lesion (types 1,2,3) – from small to large transmural, and also 1 small subepicardial lesion (type E).

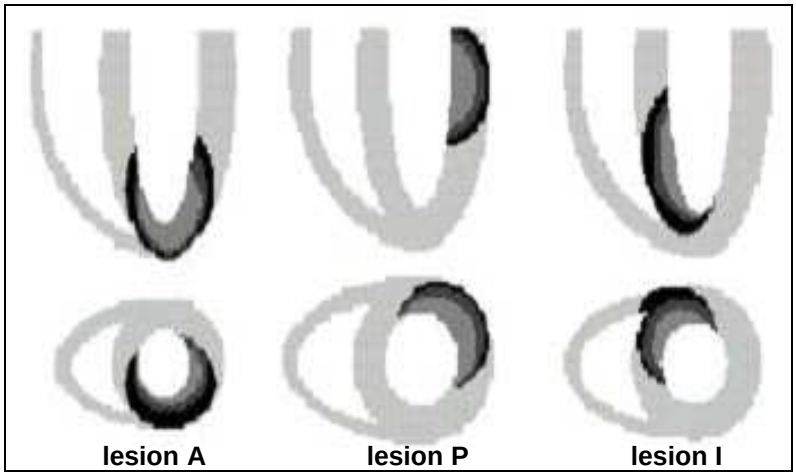

Fig.4. Simulated subendocardial regions with changed repolarization in the cross-sections of ventricular myocardium model. From left to right: antero-septal (lesion A), postero-lateral (lesion P) and inferior regions (lesion I). Top - frontal view, bottom - horizontal view. Three levels of grey color represent 3 sizes of modeled lesion from small (light grey) to large transmural (black) [9].

By solving the inverse problem we tried to reconstruct the modeled lesion from the simulated difference integral map. Computation of the difference integral map **Δp** for the model by subtracting the integral map for normal myocardium activation ($\mathbf{p}_{norm}$) from the integral map

with ischemic area ($\mathbf{p_{isch}}$) is equivalent to computation of the difference map for a difference multiple dipole integral generator **Δs**, since by linearity of the transfer matrix

$$\mathbf{A.s_{isch} = p_{isch},} \quad \mathbf{A.s_{norm} = p_{norm}} \quad \textbf{and} \quad \mathbf{\Delta p = p_{isch} - p_{norm},}$$

we have

$$\mathbf{\Delta p = A.s_{isch} - A.s_{norm} = A. (s_{isch} - s_{norm}) = A . \Delta s} \qquad \textbf{(1a)}$$

Where $\mathbf{s_{norm}}$ represents the normal generator and $\mathbf{s_{isch}}$ represents the ischemic generator.

2.4 Singular value decomposition (SVD)

Matrix **A** represents a linear operator mapping the 3m-dimensional generator space to the n-dimensional integral map space. The most common technique for finding inverse solution to the above matrix equation is SVD, which factorizes **A** into the form:

$$\mathbf{A = U \times \Sigma \times V^t ,} \qquad \textbf{(2)}$$

where $\mathbf{\Sigma = diag\{ \lambda_i \}}$ is a diagonal matrix with non-negative singular values λ_i. Columns of **V** and **U** are known as singular vectors and define orthonormal basis for the generator and integral map spaces, respectively. Since the singular vectors are unit vectors, each singular value λ_i acts as a scaling factor for generator **s** along the corresponding basis vector (i-th column of **V)** [5].

Typically, the singular values λ_i are sorted into a non-increasing series. If with increasing index **i**, λ_i approach small values**,** the inverse problem to **(1)** is ill-posed. In such cases there exists a critical index **l**, such that the contribution of basis vectors with indices **i > l** to the right hand side of **(1)** is negligible (or is in the range of noise) [4]. We will call the subspace of the 3m-dimensional generator space spanned by the columns of **V** with indices **i** > **l bad space** (or **numerical null space**). Analogically, we will call its complement in the generator space (the span of columns of **V** with indices **i** <= **l**) the **signal space**.

Since both **U** and **V** are orthonormal matrices, their inverses can be conveniently computed through transposition: $\mathbf{U^{-1} = U^t}$; $\mathbf{V^{-1} = V^t}$. Hence,

$$\mathbf{A^{-1} = V \times \Sigma^{-1} \times U^t} , \qquad \textbf{(3)}$$

where $\Sigma^{-1} = [\text{diag } (1/\lambda_i)]$.

For small values of λ_i, the expression $\mathbf{1/\lambda_i}$ becomes numerically unstable. Therefore, in practice the matrix **A** is inverted through the so called **truncated SVD,** using only singular vectors with large enough singular values (the first **l** columns of **U** and **V).** Then the solution **s'** of the inverse problem of **(1)** is expressed as the linear combination of basis vectors from signal space, i.e. it lies in the signal space. If a substantial portion of the original generator **s** lied in the bad space, the integral map **A.s** would be negligibly small, making the inverse problem infeasible. We suggested to quantify the degree of feasibility of finding the inverse solution for integral maps generated by generator **s** by the angle **α** between **s** and **s'** – its projection in the signal space (Fig. 5):

$$\mathbf{\alpha = \arccos ((s . s')/(|s| . |s'|))} \qquad \textbf{(4)}$$

where **(s . s')** is a dot product of vectors **s** and **s'** and **|s| , |s'|** are the norms of **s** and **s',** respectively.

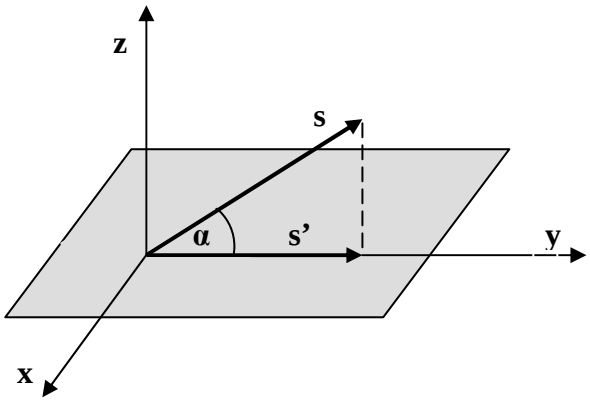

Fig.5. Schematic illustration of the relation between the modeled generator **s** and the signal space can be expressed by the angle **α**. 3D space [x,y,z] represents the space of original generator and 2D space [x,y] represents the corresponding signal space. The solution **s'** is the projection of **s** to the signal space.

3 Results

We applied SVD to the transfer matrix **A** from **(1)** (with 198 measuring points and 3x168 components of multiple dipole generator) and used 5 different values of the criterion **svdcrit** for the SVD truncation.
The **svdcrit** was defined as:

$$\textbf{svdcrit} = \lambda_l / \lambda_{max} \qquad \textbf{(4)}$$

where λ_{max} - is the biggest singular value from **(2),** λ_l – is the singular value fulfilling the condition **(4)** for certain value of **svdcrit.** By setting the value of **svdcrit** we implicitly determined the number **l** of largest singular values corresponding to the **l** basis vectors forming the signal space. The number **l** is called the effective rank of the matrix **A** for the given **svdcrit.**
We computed the angle **α** (Fig.5) for following values of **svdcrit**: 0.1; 0.01; 0.001; 0.0001 and 0.00000001**.** The results are summarized in graphs in Fig.6.

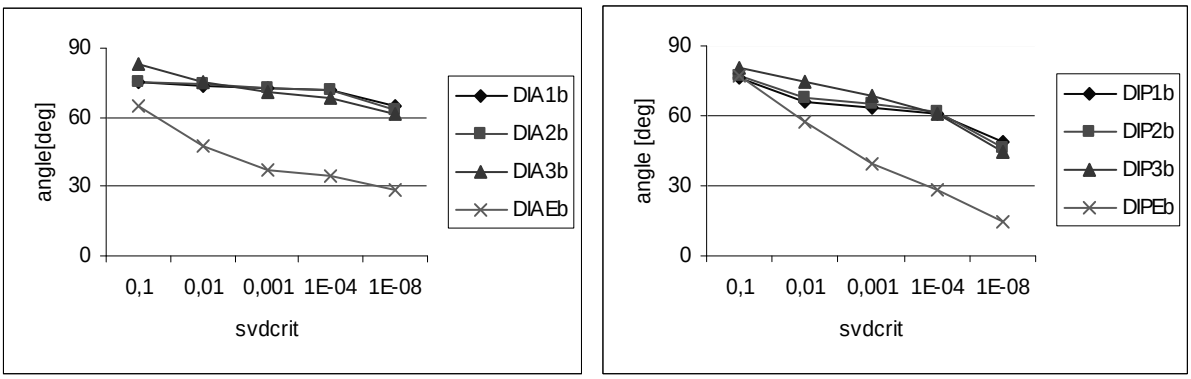

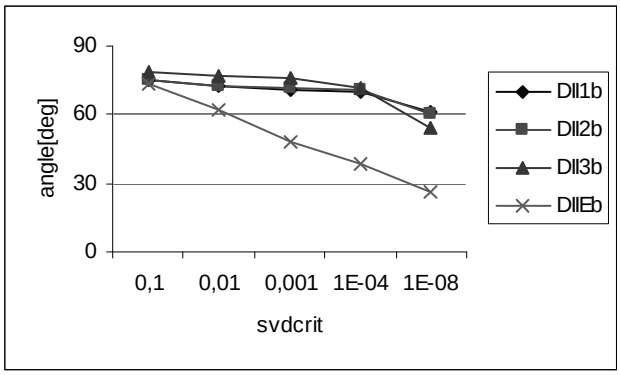

Fig.6. Computed angle **α** between the vector of modeled difference integral generator and the signal space of transfer matrix **A** for several values of **svdcrit** parameter. Top left: angle **α** for three modeled sizes of subendocardial anterior lesions from small (A1) to large transmural (A3) and one small subepicardial lesion (AE), top right: angle **α** for postero-lateral lesions (P), bottom: angle **α** for inferior lesions (I). The value of **svdcrit** = 1E-08 represents the full possible rank of the transfer matrix, i.e. the situation when the basis vectors corresponding to all nonzero values of **λ** were taken into consideration.

In the best case, **α** should be near to zero, so the whole generator can be described within the signal space, in the worst case **α** is close to 90 degrees and the projection of the generator within the signal space is negligible. For subendocardial lesions (type 1,2,3) the **α** is very high even if we chose the full possible rank of basis vectors i.e. **svdcrit** = 1E-08. The projection of the generator for subendocardial lesion A2 and subepicardial lesion AE is shown in Fig.7a and Fig.7b.

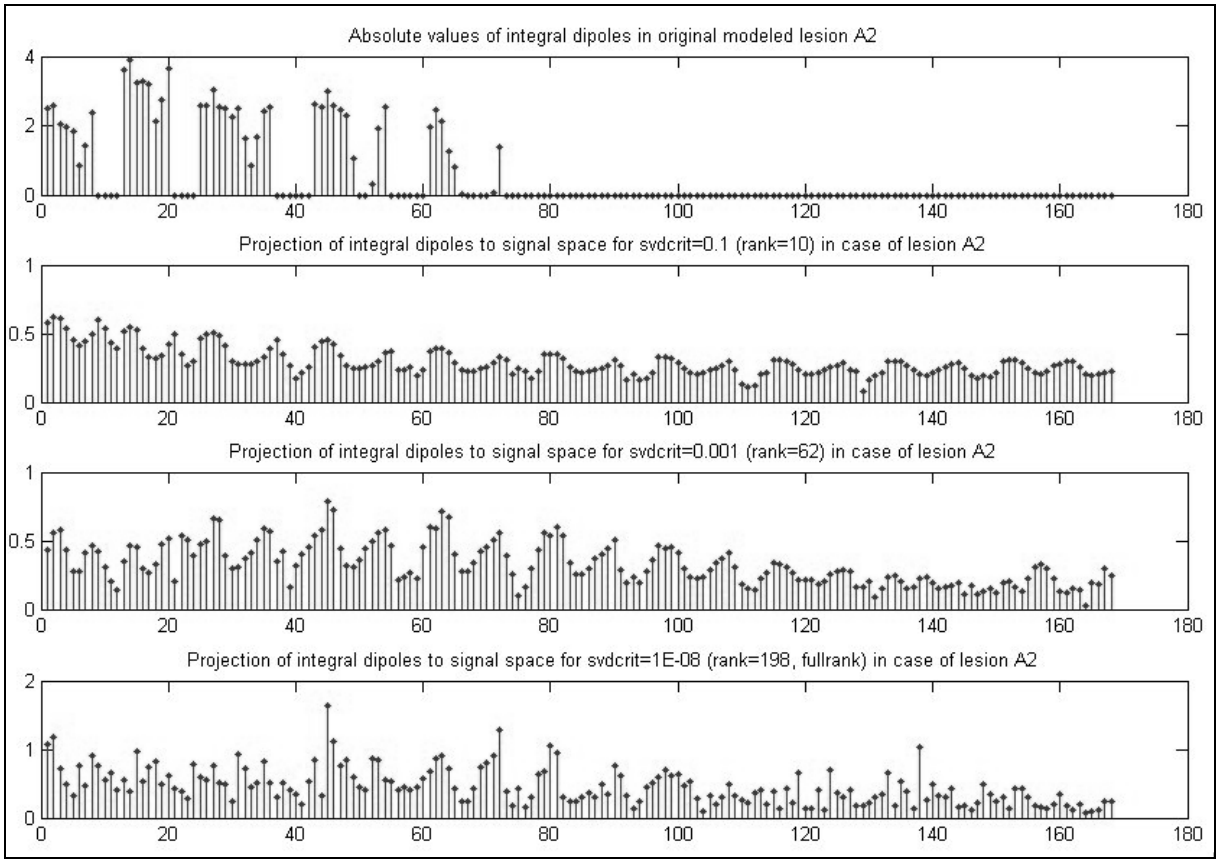

Fig.7a. Projection of the subendocardial anterior lesion A2 with large angle **α** to the signal space. Absolute values of the original reference multiple dipole model of ischemic lesion (first graph). Projections of absolute values of dipole moment integrals of the original multiple dipole model to the signal space of transfer matrix **A** for various values of parameter **svdcrit** (other graphs from top to bottom). Axis x denotes order numbers of the segments in heart generator; axis y denotes absolute values of the given integral dipole moments (in mA.m.ms)

The top graph in Fig.7a depicts the absolute values of integral dipole moments in each segment of the original difference multiple dipole equivalent generator. The following graphs (top to bottom) show projections of the generator vector **s** to the signal space of the transfer matrix **A** for different values of effective rank **l**. For subendocardial lesions (represented by A2) if **svdcrit** = 0.001, **α** is very high, **α** > 65deg. Even if **svdcrit** is very small (**svdcrit** = 1E-08; **l** = 198) it is still not possible to reconstruct the original generator (Fig. 7a), because the angle **α** remained too large **α** > 61deg. On the other hand, the projection of the original generator to the signal space for the subepicardial lesions (represented by AE) with **svdcrit** = 0.001 provides satisfactory reconstruction of the original generator (Fig. 7b), due to the considerably smaller **α, α** < 45deg (see cases AE, IE, PE in Fig 6).

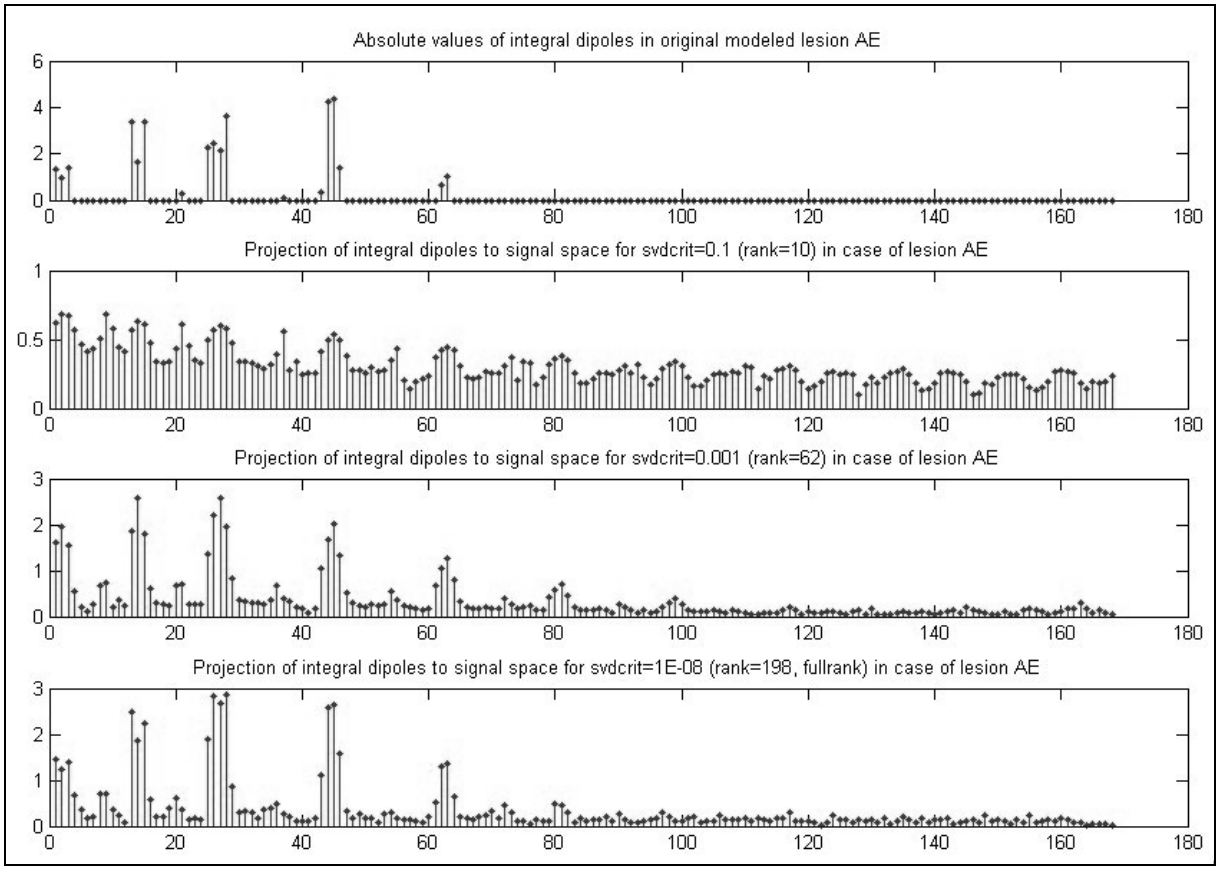

Fig.7b. Projection of the subepicardial anterior lesion AE with rather smaller angle **α** to the signal space. Absolute values of the original reference multiple dipole model of ischemic lesion (first graph). Projections of absolute values of dipole moment integrals of the original multiple dipole model to the signal space of transfer matrix **A** for various levels of parameter **svdcrit** (other graphs from top to bottom). Axis x denotes order numbers of the segments in heart generator; axis y denotes absolute values of the given integral dipole moments (in mA.m.ms).

4 Discussion and Conclusion

The present study investigated properties of the transfer matrix **A** used for the solution of forward and inverse problems in electrocardiography. The ability to reconstruct the equivalent multiple dipole model of the heart generator from the body surface potentials was investigated for ischemic lesions.

The system of equations represented by eq. **(1)** is ill-posed, therefore not all of the components of the model generator **s** are equally mapped into the body surface potentials **p**.

Using SVD of the transfer matrix **A**, a signal space of the generator can be defined. The theoretical analysis showed that the computed potentials **p** are determined mainly by the portion of the generator **s'** which lies in the signal space (Fig. 5).

We propose that in order to quantify the effectiveness / reliability of the inverse solution for a particular type of lesion, the angle **α** between a representative reference generator **s** and the portion of the generator in the signal space **s'** should be computed.

The subendocardial ischemic lesions modeled by multiple dipole model of the heart generator with 168 dipoles could not be inversely reconstructed because the vectors representing modeled lesion generators did not lie in the signal space (they were close to the nullspace) of the transfer matrix **A** (**α** >65deg – Fig. 6). Significantly better results were obtained for multiple dipole models of subepicardial lesions because the vectors representing modeled lesion generators mapped satisfactorily to the signal space of the transfer matrix **A** (**α** <45deg – Fig. 6).

In the present study the attention was focused on the signal space / nullspace of the transfer matrix **A**. However, one should keep in mind, that in practice, the inverse reconstruction of multiple dipole equivalent heart generator from real life measurements is also influenced by other important factors such as individual geometry of each patient or using limited number of measuring leads. All these factors are reflected in the specific transfer matrix.

One of the ways to avoid the ambiguity in inverse reconstruction of multiple dipole model of the cardiac electrical activity is to add some constraints or apriori information to the required generator. If we assume that the lesion is very small, (e.g. in the case of small ischemic lesions), it could be represented by a single equivalent dipole located in the area of the specific lesion [9]. Then, for every predefined position of the possible inverse dipole location we can choose the corresponding columns from the transfer matrix and solve the inverse problem by SVD of the submatrix of size [n x 3]. In most cases such submatrix has the rank of 3 (so it has no null space) and for every position we can get the unique solution of the overdetermined system of linear equations in the sense of minimum least-squares criterion. The best representative position of the single equivalent dipole was chosen using the criterion of minimal rms difference between the original difference integral map and map generated by the single dipole.

The theoretical analysis highlighted the importance of the existence of null space / signal space in every model described by a linear matrix equation. Before any attempt to analyze real data, analysis of the properties of the transfer matrix **A** can contribute to better understanding and evaluation of inverse results.

Acknowledgements

This work was supported by grants 2/7092/27 from the VEGA grant agency, APVV-51-059005 from the APVV agency and grant GVOP 3.1.1-2004-05-0196/3.0.

JS would like to thank Peter Tino (University of Birmingham, UK) for stimulating discussions and helpful consultations in preparing this paper.

References

1. Messinger-Rapport B.J., Rudy Y.:The inverse problem in electrocardiography: A model study of the effects of geometry and conductivity parameters on the reconstruction of epicardial potentials; IEEE Trans. on BME, 1986, vol. 33, pp.667-676.
2. Oosterom A. van: Source models in inverse electrocardiography. International Journal of Bioelectromagnetism, 2003, Vol.5, pp. 211-214.
3. Fisher G., Tilg B., Modre R., Huiskamp G.J., Fetzer J., Rucker W., Wach P.: A bidomain model based FEM-BEM coupling formulation for anisotropic cardiac tissue; Ann. Biomed. Eng., 2000, vol.28, pp. 1229-1243.
4. Messnarz B., Seger M., Modre R., Fisher G., Hanser F., Tilg B.: A comparison of noninvasive reconstruction of epicardial versus transmembrane potentials in consideration of the null space; IEEE Trans. on BME, 2004, vol.51, pp. 1609 – 1618
5. Golub G.H., Van Loan Ch.F.: Matrix Computations; 1983, Baltimore: John Hopkins University Press.
6. Szathmary V., Osvald R.: An interactive computer model of propagated activation with analytically defined geometry of ventricles; Computers and Biomedical Research, 1994, vol.27, pp. 27 - 38.
7. Durrer D., van Dam R.T., Freud G.E., Janse M., Meijler F.L., Arzbaecher R.C.: Total excitation of the isolated human heart; Circulation, 1970, vol. 41, pp.899 – 930.
8. Pullan A.J., Buist M.L., Cheng L.K.: Mathematically modelling the electrical activity of the heart, World Scientific 2005, p.311.
9. Tysler M., Turzova M., Tinova M., Svehlikova J., Heblakova E., Szathmary V., Filipova S.: Use of body surface potential maps for model-based assessment of local pathological changes in the heart; Bulletin of Polish Academy of Sciences, Technical Sciences, 2005, vol.53, No.3, pp. 207 – 215.
10. Tysler M., Szathmary V., Turzova M.: Model study of assessment of local heart repolarization changes by several ECG methods; Int. J. Bioelectromagnetism, 2003, vol.5, pp. 252 – 253.
11. Trudel M.C., Dube B., Potse M., Gulrajani R.M., Leon L.J.: Simulation of QRST integral maps with a membrane-based computer heart model employing parallel processing; IEEE Trans. on BME, 2004, vol.51, pp. 1319 – 1329.

Address for correspondence.

Jana Švehlíková
Institute of Measurement Science, Slovak Academy of Sciences,
Dúbravská cesta 9, 841 04 Bratislava, Slovakia
svehlikova@savba.sk